

# Anisotropic Stars: Exact Solutions

Krsna Dev and Marcelo Gleiser

*Department of Physics and Astronomy, Dartmouth College, Hanover, NH 03755 USA.*

## Abstract

We study the effects of anisotropic pressure on the properties of spherically symmetric, gravitationally bound objects. We consider the full general-relativistic treatment of this problem and obtain exact solutions for various forms of the equation of state connecting the radial and tangential pressures. It is shown that pressure anisotropy can have significant effects on the structure and properties of stellar objects. In particular, the maximum value of  $2M/R$  can approach unity ( $2M/R < 8/9$  for isotropic objects) and the surface redshift can be arbitrarily large.

## I. INTRODUCTION

A common assumption in the study of stellar structure and evolution is that the interior of a star can be modeled as a perfect fluid [1,2]. This perfect fluid model necessarily requires that the pressure in the interior of a star to be isotropic. This approach has been used extensively in the study of polytropes, including white dwarfs, and of compact objects such as neutron stars [3]. However, theoretical advances in the last decades indicate that, in many systems, deviations from local isotropy in the pressure, in particular at very high densities, may play an important role in determining their properties [4,5].

The physical situations where anisotropic pressure may be relevant are very diverse. By anisotropic pressure we mean that the radial component of the pressure,  $p_r(r)$ , differs from the angular components,  $p_\theta(r) = p_\varphi(r) \equiv p_t(r)$ . (That  $p_\theta(r) = p_\varphi(r)$  is a direct consequence

of spherical symmetry.) Of course, spherical symmetry demands both to be strictly a function of the radial coordinate. A scalar field with non-zero spatial gradient is an example of a physical system where the pressure is clearly anisotropic. [This anisotropic character of a scalar field occurs already at the level of special relativity, where it is easy to show that  $p_r - p_t = (d\phi/dr)^2$ ]. Boson stars, hypothetical self-gravitating compact objects resulting from the coupling of a complex scalar field to gravity, are systems where anisotropic pressure occurs naturally [6]. Similarly, the energy-momentum tensor of both electromagnetic and fermionic fields are naturally anisotropic. Isotropy appears as an extra assumption on the behaviors of the fields or of the fluid modeling the stellar interior.

In the interior of neutron stars pions may condense. It has been shown that due to the geometry of the  $\pi^-$  modes, anisotropic distributions of pressure could be considered to describe a pion condensed phase configuration [7]. The existence of solid cores and type P superfluidity may also lead to departures from isotropy within the neutron star interior [3]. Since we still do not have a detailed microscopic formulation of the possible anisotropic stresses emerging in these and other contexts, we take the general approach of finding several exact solutions representing different physical situations, modeled by *ansatze* for the anisotropy factor,  $p_t - p_r$ . As a general rule, we find that the presence of anisotropy affects the critical mass for stability,  $2M/R$ , and the surface redshift,  $z_s$ . These physical consequences of pressure anisotropy are not new. Previous studies have found some exact solutions, assuming certain relations for the anisotropy factor [8–14]. Our goal here is to extend those results, offering a detailed analysis of the changes in the physical properties of the stellar objects due to the presence of anisotropy. Hopefully, our results will be of importance in the analysis of data from compact objects, as well as in the study of the behavior of matter under strong gravitational fields.

This paper is organized as follows. In the next section, we set up the equations used and the assumptions made in our study. We restrict our exact solutions to two classes, investigated in sections III and IV respectively. In section III, after reviewing the results of Bowers and Liang [8], we obtain several new exact solutions for stars of constant density.

In section IV, we examine solutions for the case  $\rho(r) \propto 1/r^2$ , which has been used to model ultradense neutron star interiors [15]. We conclude in section V with a brief summary of our results and an outlook to future work. In Appendix A, we demonstrate the equivalence of the Tolman and Schwarzschild masses for self-gravitating anisotropic spheres. In Appendix B we present the general solution for stars featuring an energy density with a constant part and a  $r^{-2}$  contribution, as discussed in Section IV, in terms of hypergeometric functions.

## II. RELATIVISTIC SELF-GRAVITATING SPHERES

We consider a static equilibrium distribution of matter which is spherically symmetric. In Schwarzschild coordinates the metric can be written as

$$ds^2 = e^\nu dt^2 - e^\lambda dr^2 - r^2 d\theta^2 - r^2 \sin^2 \theta d\phi^2 , \quad (1)$$

where all functions depend only on the radial coordinate  $r$ . The most general energy-momentum tensor compatible with spherical symmetry is

$$T_\nu^\mu = \text{diag}(\rho, -p_r, -p_t, -p_t) . \quad (2)$$

We see that isotropy is not required by spherical symmetry; it is an added assumption. The Einstein field equations for this spacetime geometry and matter distribution are

$$e^{-\lambda} \left( \frac{\nu'}{r} + \frac{1}{r^2} \right) - \frac{1}{r^2} = 8\pi p_r ; \quad (3)$$

$$e^{-\lambda} \left( \frac{1}{2} \nu'' - \frac{1}{4} \lambda' \nu' + \frac{1}{4} (\nu')^2 + \frac{(\nu' - \lambda')}{2r} \right) = 8\pi p_t ; \quad (4)$$

$$e^\lambda \left( \frac{\lambda'}{r} - \frac{1}{r^2} \right) + \frac{1}{r^2} = 8\pi \rho . \quad (5)$$

Note that this is a system of 3 equations with 5 unknowns. Consequently, it is necessary to specify two equations of state, such as  $p_r = p_r(\rho)$  and  $p_t = p_t(\rho)$ .

It is often useful to transform the above equations into a form where the hydrodynamical properties of the system are more evident. For systems with isotropic pressure, this formulation results in the Tolman-Oppenheimer-Volkov (TOV) equation. The generalized TOV equation, including anisotropy, is

$$\frac{dp_r}{dr} = -(\rho + p_r)\frac{\nu'}{2} + \frac{2}{r}(p_t - p_r) , \quad (6)$$

with

$$\frac{1}{2}\nu' = \frac{m(r) + 4\pi r^3 p_r}{r(r - 2m)} , \quad (7)$$

and

$$m(r) = \int_0^r 4\pi r'^2 \rho dr' . \quad (8)$$

Taking  $r = R$  in the above expression gives us the Schwarzschild mass,  $M$ . [This implicitly assumes that  $\rho = 0$  for  $r > R$ .]

A more general formula is the Tolman mass formula [16]:

$$M = \int_0^R (2T_0^0 - T_\mu^\mu)(-g)^{\frac{1}{2}} r^2 dr. \quad (9)$$

The equivalence of the Tolman and Schwarzschild masses for systems with anisotropic pressure is demonstrated in Appendix A.

In order to solve the above equations we must impose appropriate boundary conditions. We require that the solution be regular at the origin. This imposes the condition that  $m(r) \rightarrow 0$  as  $r \rightarrow 0$ . If  $p_r$  is finite at the origin then  $\nu' \rightarrow 0$  as  $r \rightarrow 0$ . The gradient  $dp_r/dr$  will be finite at  $r = 0$  if  $(p_t - p_r)$  vanishes at least as rapidly as  $r$  when  $r \rightarrow 0$ . This will be the case in all scenarios examined here.

The radius of the star is determined by the condition  $p_r(R) = 0$ . It is not necessary for  $p_t(R)$  to vanish at the surface. But it is reasonable to assume that all physically interesting solutions will have  $p_r, p_t \geq 0$  for  $r \leq R$ .

### III. EXACT SOLUTIONS FOR $\rho = \text{CONSTANT}$

For  $\rho \equiv \rho_0 = \text{constant}$ , we can write the generalized TOV equation as

$$\frac{dp_r}{dr} = \frac{2}{r}(p_t - p_r) - \frac{4\pi r(p_r^2 + \frac{4}{3}p_r\rho_0 + \frac{\rho_0^2}{3})}{1 - \frac{8}{3}\pi\rho_0 r^2}. \quad (10)$$

Bowers and Liang [8] solved the generalized TOV equation by considering the following equation of state,

$$p_t - p_r = C \frac{r^2(p_r^2 + \frac{4}{3}p_r\rho_0 + \frac{\rho_0^2}{3})}{1 - \frac{8}{3}\pi\rho_0 r^2}, \quad (11)$$

that is, they considered the term related to the anisotropy to be simply proportional to the usual hydrodynamic term on the right hand side. The constant parameter  $C$ , which we will also use, measures the amount of anisotropy.

They found that the radial pressure is given by

$$p_r = \rho_0 \left[ \frac{(1 - 2m/r)^Q - (1 - 2M/R)^Q}{3(1 - 2M/R)^Q - (1 - 2m/r)^Q} \right], \quad (12)$$

where the total mass  $M \equiv m(R)$ ,  $R$  is the radius of the system, and  $Q = \frac{1}{2} - \frac{3C}{4\pi}$ . The central pressure is given by

$$p_c = \rho_0 \left[ \frac{1 - (1 - 2M/R)^Q}{3(1 - 2M/R)^Q - 1} \right]. \quad (13)$$

An equilibrium configuration exists for all values of  $2M/R$  such that  $p_c$  is finite. The critical model results for that value of  $2M/R$  such that  $p_c$  becomes infinite. From eq. 13, this occurs when the denominator vanishes, that is, when

$$(2M/R)_{\text{crit}} = 1 - \left(\frac{1}{3}\right)^{\frac{2}{1-\xi}}, \quad (14)$$

where  $\xi \equiv 3C/2$ . We see that for  $0 \leq \xi < 1$ ,  $(2M/R)_{\text{crit}}$  can be greater than  $8/9$ , the maximum value for an isotropic configuration [15]. For a given  $\rho_0$  and  $C$ , the critical mass is

$$M_{\text{crit}} = \left(\frac{3}{32\pi\rho_0}\right)^{\frac{1}{2}} \left[1 - \left(\frac{1}{3}\right)^{\frac{2}{1-\xi}}\right]^{\frac{3}{2}}. \quad (15)$$

Equation 15 shows that the critical mass is less than the isotropic value when  $C < 0$ . When  $C > 0$  the critical mass exceeds the isotropic limit. For a given  $\rho_0$ , the maximum value of the ratio of the critical mass to the isotropic mass approaches

$$M_a(\xi = 1)/M_i \simeq 1.19 , \quad (16)$$

where  $M_a(\xi = 1)$  corresponds to a configuration uniformly filling up to its own Schwarzschild radius. This represents a maximum of 19% increase in the stable mass, comparable with results for relativistic models of slowly rotating isotropic stars [17]. The increase in stellar mass also affects the surface redshift,

$$z_s = (1 - 2M/R)^{-\frac{1}{2}} - 1 . \quad (17)$$

For the Bowers-Liang solution, the maximum redshift is,

$$z_c = 3^{\frac{1}{1-\xi}} - 1. \quad (18)$$

For  $\xi = 0$  we recover the well-known isotropic result  $z_c = 2$ . The introduction of anisotropy removes the upper limit, since as  $\xi \rightarrow 1$ ,  $z_c$  can be arbitrarily large. Thus, in principle, a modest amount of anisotropy is capable of explaining surface redshifts greater than 2, an intriguing possibility.

For stars with constant energy density  $\rho_0$ , we considered solutions to two general *ansatze*, which we label cases I and II for convenience. We begin with case I:

**CASE I:** The anisotropy factor is written as

$$p_t - p_r = Cr^2 F(p_r, \rho_0) \left(1 - \frac{8}{3}\pi\rho_0 r^2\right)^{-1} , \quad (19)$$

where  $C$  measures the amount of anisotropy and the function  $F(p_r, \rho_0)$  includes 6 separate cases,

$$F = (p_r^2; p_r\rho_0; \rho_0^2; p_r^2 + p_r\rho_0; p_r^2 + \rho_0^2; p_r\rho_0 + \rho_0^2) . \quad (20)$$

For the sake of brevity, we will only discuss 2 of the 6 possible cases. It should be straightforward to obtain solutions for the other cases.

**Case I.1**  $F(p_r, \rho_0) = \rho_0^2$

When  $F(p_r, \rho_0) = \rho_0^2$  the *TOV* equation becomes

$$\frac{dp_r}{dr} = -\frac{4\pi r \left[ p_r^2 + \frac{4}{3}p_r\rho_0 + \left(\frac{1}{3} - \frac{C}{2\pi}\right)\rho_0^2 \right]}{1 - \frac{8}{3}\pi\rho_0 r^2}. \quad (21)$$

Thus we find

$$\int_0^{p_r} \frac{dp_r}{\left[ p_r^2 + \frac{4}{3}p_r\rho_0 + \left(\frac{1}{3} - \frac{C}{2\pi}\right)\rho_0^2 \right]} = -4\pi \int_R^r \frac{dr}{1 - \frac{8}{3}\pi\rho_0 r^2}. \quad (22)$$

The solutions naturally divide into 3 subcases, according to the value of the anisotropy parameter, which we write as  $k \equiv C/(2\pi)$ .

When  $k > -1/9$  the radial pressure is given by

$$p_r(r) = \rho_0 \left[ \frac{(1 - 3k)[(1 - 2m/r)^{\frac{A}{2}} - (1 - 2M/R)^{\frac{A}{2}}]}{(2 + A)(1 - 2M/R)^{\frac{A}{2}} - (2 - A)(1 - 2m/r)^{\frac{A}{2}}} \right], \quad (23)$$

where  $A \equiv (1 + 9k)^{\frac{1}{2}}$ . Clearly, when  $k = 0$  we recover the isotropic limit. In figure 1.1, we show the radial pressure as a function of the radius parameterized in terms of fractions of the critical configuration,  $(2M/R)_{\text{crit}}$ . The solutions are normalized to  $p_r(R) = 0$ . Alternatively, to obtain a solution we can fix  $\rho_0$  and  $p_c$ , the central pressure, and compute the value of  $r$  for which  $p_r(R) = 0$ .

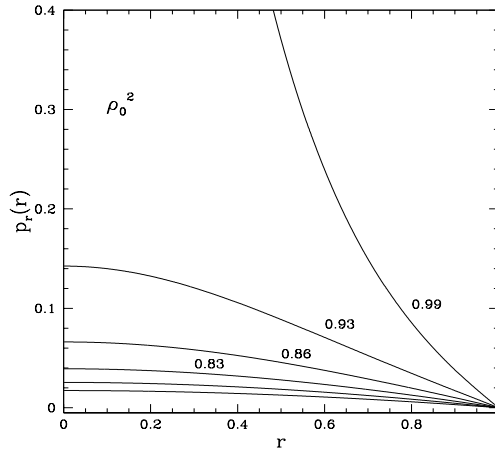


Fig. 1.1: Radial pressure as a function of radius for the case  $k = 1/2\pi$ ,  $\rho = \text{const}$  and  $(p_t - p_r) \propto \rho^2$  parameterized in terms of fractions of the critical configuration  $(2M/R)_{\text{crit}}$ .

The central pressure is given by

$$p_c = \rho_0 \left[ \frac{(1-3k)[1-(1-2M/R)^{\frac{A}{2}}]}{(2+A)(1-2M/R)^{\frac{A}{2}} - (2-A)} \right] . \quad (24)$$

Thus, for  $k > -1/9$  we obtain,

$$\left(\frac{2M}{R}\right)_{\text{crit}} = 1 - \left[\frac{(2-A)}{(2+A)}\right]^{\frac{2}{A}} . \quad (25)$$

For  $|k| \ll 1$  we find that, correcting slightly Bowers and Liang [8],

$$\left(\frac{2M}{R}\right)_{\text{crit}} \simeq \frac{8}{9} + \left(\frac{4}{3} - \ln 3\right)k + \mathcal{O}(k^2) . \quad (26)$$

We see that a positive anisotropy,  $k > 0$ , leads to a violation of the isotropic limit  $(2M/R)_{\text{crit}} = 8/9$ . However, as  $k \rightarrow 1/3$ ,  $(2M/R)_{\text{crit}} \rightarrow 1$  and  $p_r < 0$ : there is a maximum allowed anisotropy in this case. When  $k < 0$ ,  $(2M/R)_{\text{crit}}$  is always less than  $8/9$ .

The maximum surface redshift for  $k > -1/9$  is

$$z_c = \left(\frac{2+A}{2-A}\right)^{\frac{1}{A}} - 1 . \quad (27)$$

For  $k = -1/9$ , the radial pressure is

$$p_r(r) = \frac{2}{3}\rho_0 \left[ \frac{1}{1 - \frac{1}{2}\ln\left(\frac{1-2m/r}{1-2M/R}\right)} - 1 \right] . \quad (28)$$

This matches smoothly the result for  $k > -1/9$ , as  $k \rightarrow -1/9$ .

When  $k < -1/9$  the radial pressure is given by

$$p_r(r) = \frac{\rho_0}{3} \left\{ B \tan \left[ \arctan \left( \frac{2}{B} \right) + \frac{B}{4} \left( \ln \left( \frac{1-2m/r}{1-2M/R} \right) \right) \right] - 2 \right\} , \quad (29)$$

with  $B \equiv (9|k| - 1)^{\frac{1}{2}}$ . Now, the central pressure is

$$p_c = \frac{\rho_0}{3} \left[ B \tan \left( \arctan \left( \frac{2}{B} \right) - \frac{B}{4} \ln(1-2M/R) \right) - 2 \right] , \quad (30)$$

and the critical values of  $2M/R$  are

$$\left(\frac{2M}{R}\right)_{\text{crit}} = 1 - \exp \left[ \frac{4}{B} \arctan \left( \frac{2}{B} \right) - \frac{\pi}{2} \right] . \quad (31)$$

In figure 1.2, we plot the critical values of  $2M/R$  as a function of the anisotropic parameter  $C$ .



The maximum surface redshift for  $k < -1/9$  is

$$z_c = \exp \left[ \frac{\pi}{4} - \frac{2}{B} \arctan\left(\frac{2}{B}\right) \right] - 1 . \quad (32)$$

In figure 1.3, we plot the maximum surface redshift as a function of the anisotropic parameter  $C$ . We find that for  $A \rightarrow 2$ , *i.e.*,  $k \rightarrow 1/3$ , the surface redshift becomes infinite. Thus, in this model, positive anisotropies generate arbitrarily large surface redshifts.

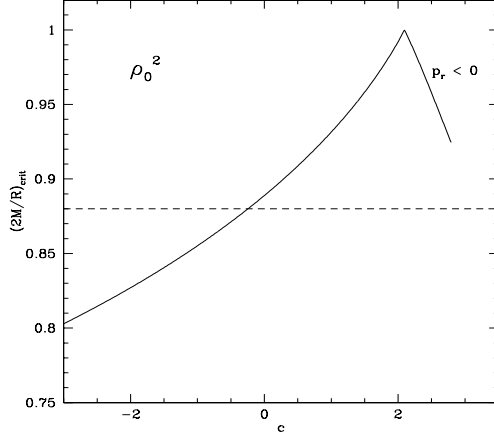


Fig. 1.2 Critical values of  $2M/R$  as a function of the anisotropic parameter  $C$  for the case  $\rho = \text{const}$  and  $(p_t - p_r) \propto \rho^2$ .

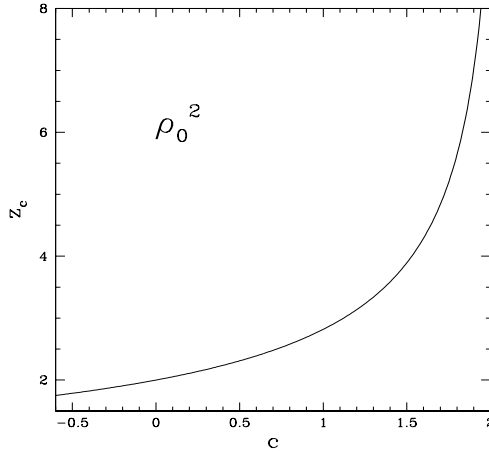


Fig 1.3: Maximum surface redshift as a function of the anisotropic parameter  $C$  for the case  $\rho = \text{const}$  and  $(p_t - p_r) \propto \rho^2$ .

**Case I.2:**  $F(p_r, \rho_0) = p_r^2$

This solution also separates into 3 subcases, depending on the value of the anisotropy parameter,  $k = C/(2\pi)$ . When  $k > -1/3$ , the radial pressure is given by

$$p_r(r) = \rho_0 \left[ \frac{(1 - 3k)[(1 - 2m/r)^{\frac{A}{2}} - (1 - 2M/R)^{\frac{A}{2}}]}{(2 + A)(1 - 2M/R)^{\frac{A}{2}} - (2 - A)(1 - 2m/r)^{\frac{A}{2}}} \right] , \quad (33)$$

where  $A \equiv (1 + 3k)^{\frac{1}{2}}$ . In figure 2.1, we show the radial pressure as a function of the radial coordinate for fractions of  $(2M/R)_{\text{crit}}$  and  $k = 1/\pi$ .

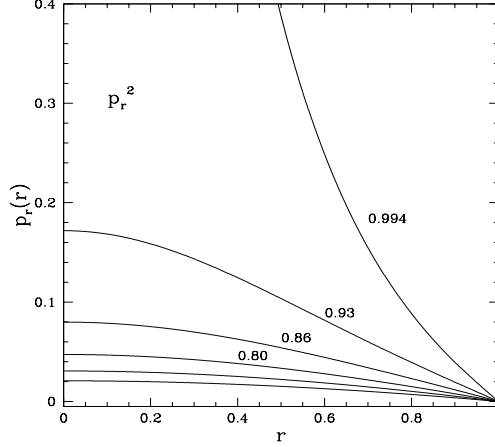


Fig 2.1: Radial pressure as a function of radius for the case  $k = 1/\pi$ ,  $\rho = \text{const}$  and  $(p_t - p_r) \propto p_r^2$  parameterized in terms of fractions of the critical configuration  $(2M/R)_{\text{crit}}$ .

The central pressure is given by

$$p_c = \rho_0 \left[ \frac{(1 - 3k)[1 - (1 - 2M/R)^{\frac{A}{2}}]}{(2 + A)(1 - 2M/R)^{\frac{A}{2}} - (2 - A)} \right]. \quad (34)$$

The critical configurations for the anisotropy parameter  $k > -1/3$  are given by

$$\left( \frac{2M}{R} \right)_{\text{crit}} = 1 - \left[ \frac{(2 - A)}{(2 + A)} \right]^{\frac{2}{A}}, \quad (35)$$

and the corresponding maximum redshift for these values of  $k$  are

$$z_c = \left[ \frac{(2 + A)}{(2 - A)} \right]^{\frac{1}{A}} - 1. \quad (36)$$

For  $k = -1/3$ , the radial pressure is given by

$$p_r(r) = \rho_0 \left[ \frac{1}{2 - \ln\left(\frac{1-2m/r}{1-2M/R}\right)} - \frac{1}{2} \right], \quad (37)$$

and the central pressure is

$$p_c = \rho_0 \left[ \frac{1}{2 + \ln(1 - 2M/R)} - \frac{1}{2} \right]. \quad (38)$$

Thus, for  $k = -1/3$  we have

$$\left( \frac{2M}{R} \right)_{\text{crit}} = 1 - e^{-2}. \quad (39)$$

The solution for  $k < -1/3$  is

$$p_r(r) = \frac{\rho_0}{3(1-k)} \left\{ B \tan \left[ \arctan \left( \frac{2}{B} \right) + \frac{B}{4} \ln \left( \frac{1-2m/r}{1-2M/R} \right) \right] - 2 \right\} , \quad (40)$$

with  $B \equiv (3|k| - 1)^{\frac{1}{2}}$ . The central pressure is

$$p_c = \frac{\rho_0}{3(1-k)} \left[ B \tan \left( \arctan \left( \frac{2}{B} \right) - \frac{B}{4} \ln(1-2M/R) \right) - 2 \right] . \quad (41)$$

Now,

$$\left( \frac{2M}{R} \right)_{\text{crit}} = 1 - \exp \left[ \frac{4}{B} \arctan \left( \frac{2}{B} \right) - \frac{\pi}{2} \right] , \quad (42)$$

and the corresponding maximum surface redshift is

$$z_c = \exp \left[ \frac{\pi}{4} - \frac{2}{B} \arctan \left( \frac{2}{B} \right) \right] - 1 . \quad (43)$$

Note that the critical values of  $2M/R$  and surface redshifts for cases I.1 and I.2 are identical, up to a shift in  $k \rightarrow k/3$ . In figures 2.2 and 2.3 we plot the critical values of  $2M/R$  and the maximum surface redshift as a function of the anisotropic parameter  $C$ .

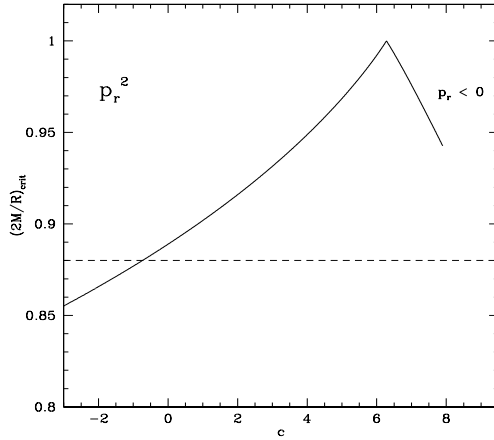


Fig 2.2: Critical values of  $2M/R$  as a function of the anisotropic parameter  $C$  for the case  $\rho = \text{const}$  and  $(p_t - p_r) \propto p_r^2$ .

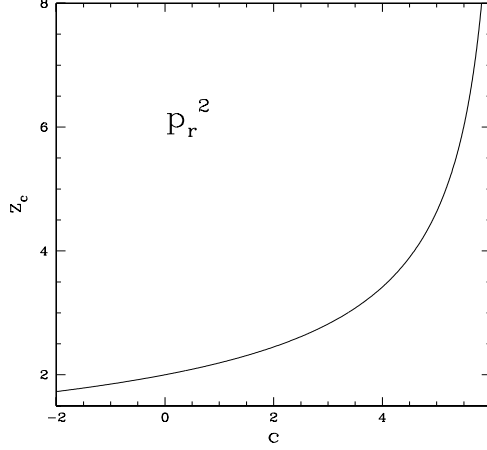


Fig 2.3: Maximum surface redshift as a function of the anisotropic parameter  $C$  for the case  $\rho = \text{const}$  and  $(p_t - p_r) \propto p_r^2$ .

## CASE II

The second class of exact solutions with constant density follows the *ansatze*,

$$p_t - p_r = \frac{C \frac{r^n}{R^n} \exp(-\frac{r}{R})(p_r^2 + \frac{4}{3}p_r\rho_0 + \frac{\rho_0^2}{3})}{\rho_0 \left(1 - \frac{8}{3}\pi\rho_0 r^2\right)}, \quad (44)$$

and

$$p_t - p_r = \frac{C \frac{r^n}{R^n} \exp(-\frac{r^2}{R^2})(p_r^2 + \frac{4}{3}p_r\rho_0 + \frac{\rho_0^2}{3})}{\rho_0 \left(1 - \frac{8}{3}\pi\rho_0 r^2\right)}, \quad (45)$$

where  $n \geq 2$  is an integer. The motivation for this choice of anisotropy comes from boson stars [6], where it is found that the anisotropy factor vanishes at the origin and outside the star, reaching a maximum somewhere around the approximate radius of the configuration. (Boson stars do not have a sharp boundary between the inside and the outside, as the scalar field vanishes exponentially for  $r > R$ . One may think of it as a diffuse “atmosphere” around the denser stellar core.)

For all cases considered, we found that there are values of  $C > 0$  for which  $(2M/R)_{\text{crit}}$  can be greater than  $8/9$  and  $z_c$  can approach arbitrarily large values. Let us focus on the case where the anisotropy falls exponentially with distance, as in eq. 44. The case for the “Gaussian” anisotropy (eq. 45) can be solved by following the same procedure. After integration we obtain,

$$p_r(r) = \rho_0 \frac{Z(r) - 1}{3 - Z(r)} , \quad (46)$$

where

$$Z(r) \equiv \left( \frac{1 - 8\pi\rho_0 r^2/3}{1 - 8\pi\rho_0 R^2/3} \right)^{\frac{1}{2}} \exp \left[ \frac{4C}{3R^n} \int_R^r r'^{(n-1)} \exp(-r'/R) dr' \right] . \quad (47)$$

For a given  $n$  the integral can be easily performed and we obtain an expression for the radial pressure. Note that for physically acceptable solutions (*i.e.*, with  $p_r(r) > 0$ ) the function  $Z(r)$  must satisfy  $1 \leq Z(r) \leq 3$ . In figure 3.1 we show the radial pressure as a function of radial distance for various fractions of  $(2M/R)_{\text{crit}}$  and  $n = 2$ . In figure 3.2, we plot the anisotropy factor for the same fractions of  $(2M/R)_{\text{crit}}$  and  $n = 2$ .

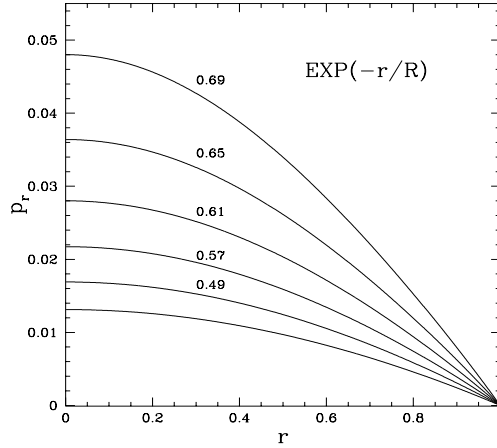


Fig. 3.1: Radial pressure as a function of radius for the case  $\rho = \text{const}$  and  $p_t - p_r \propto (\frac{r}{R})^2 \exp(-\frac{r}{R})$  parameterized in terms of fractions of the critical configuration  $(2M/R)_{\text{crit}}$ .

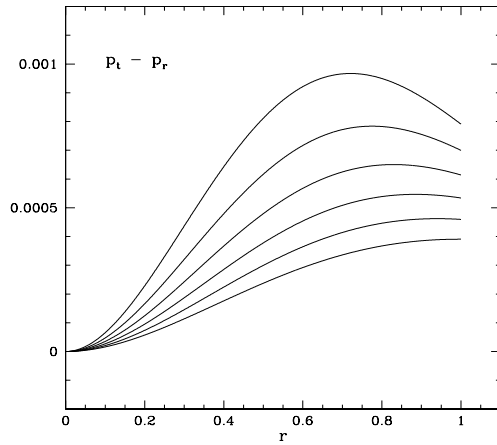


Fig. 3.2: Anisotropy factor as a function of the radius for the same case as in fig. 3.1.

Of more interest is the behavior at the origin. From the above solution, the central pressure can be written as,

$$p_c = \rho_0 \frac{Z(0) - 1}{3 - Z(0)}, \quad (48)$$

where

$$Z(0) = \left(1 - 8\pi\rho_0 R^2\right)^{-1/2} \exp \left[ \frac{4C}{3R^n} \int_R^0 r'^{(n-1)} \exp(-r'/R) dr' \right]. \quad (49)$$

The critical configuration is obtained for  $Z(0) = 3$ . For example, for  $n = 2$  we obtain,

$$\left(\frac{2M}{R}\right)_{\text{crit}} = 1 - \frac{1}{9} \exp \left[ -\frac{8C}{3} (1 - 2e^{-1}) \right]. \quad (50)$$

Note that, as  $C \rightarrow \infty$ ,  $(2M/R)_{\text{crit}} \rightarrow 1$ : there is no maximum positive anisotropy. On the other hand, there is a maximum negative anisotropy, beyond which the central pressure becomes negative ( $Z(0) < 1$ ). This is given by  $|C| = \frac{3}{8(1-2e^{-1})} \ln 9 \simeq 3.12$ . In the Introduction, we noted that boson stars have negative pressure anisotropy,  $p_t - p_r < 0$ . It is an interesting open question if such “exploding” solutions with negative core pressures represent a new kind of instability of bosonic stellar configurations.

In figure 3.3 we plot the critical mass as a function of anisotropy, for several values of  $n$ . In figure 3.4 we do the same for the surface redshift. For  $n = 2$  the surface redshift is given by,

$$z_c = 3 \exp \left[ \frac{4C}{3} (1 - 2e^{-1}) \right] - 1. \quad (51)$$

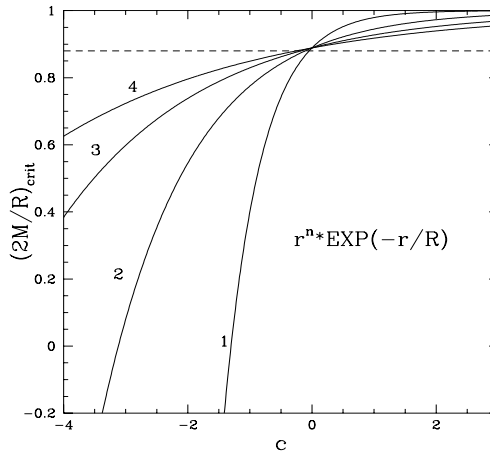


Fig. 3.3: Critical values of  $2M/R$  as a function of anisotropy for the case  $\rho = \text{const}$  and  $p_t - p_r \propto \left(\frac{r}{R}\right)^n \exp\left(-\frac{r}{R}\right)$  with  $n = 1, 2, 3, 4$ .

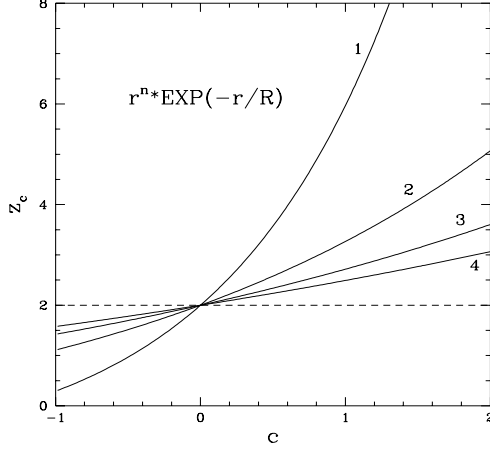


Fig. 3.4: Maximum surface redshift as a function of anisotropy for the case  $\rho = \text{const}$  and  $p_t - p_r \propto \left(\frac{r}{R}\right)^n \exp\left(-\frac{r}{R}\right)$ , with  $n = 1, 2, 3, 4$ .

#### IV. EXACT SOLUTIONS FOR $\rho \propto 1/r^2$

We will now consider anisotropic stellar configurations with the following expression for the energy density

$$\rho = \frac{1}{8\pi} \left( \frac{a}{r^2} + 3b \right), \quad (52)$$

where both  $a$  and  $b$  are constant. The choice of the values for  $a$  and  $b$  is dictated by the physical configuration under consideration. For example,  $a = 3/7$  and  $b = 0$ , corresponds to a relativistic Fermi gas. If we take  $a = 3/7$  and  $b \neq 0$  then we have a relativistic Fermi gas core immersed in a constant density background. For large  $r$  the constant density term dominates ( $r_c^2 \gg a/3b$ ), and can be thought of as modeling a shell surrounding the core.

In this section we will consider cases where the pressure anisotropy closely resembles the behavior of the energy density. Hence we will take

$$p_t - p_r = \frac{1}{8\pi} \left( \frac{c}{r^2} + d \right), \quad (53)$$

with  $c$  and  $d$  constant. The motivation for these ansatze comes from similar approaches used to model the equation of state of ultradense neutron stars [4,5].

We have found it convenient to seek solutions for the metric function  $\nu(r)$  directly, rather than solving the generalized TOV equation. We will then use the known functions  $\lambda(r)$  and  $\nu(r)$  to find the radial and tangential pressures. From eqs. 3, 4, and 5, we find

$$\left(\frac{\nu''}{2} + \frac{(\nu')^2}{4}\right) e^{-\lambda} - \nu' \left(\frac{\lambda'}{4} + \frac{1}{2r}\right) e^{-\lambda} - \left(\frac{1}{r^2} + \frac{\lambda'}{2r}\right) e^{-\lambda} + \frac{1}{r^2} = 8\pi(p_t - p_r). \quad (54)$$

Introducing a new variable  $y = e^{\frac{\nu}{2}}$ , eq. 54 becomes,

$$(y'')e^{-\lambda} - y' \left(\frac{\lambda'}{2} + \frac{1}{r}\right) e^{-\lambda} - y \left[\left(\frac{1}{r^2} + \frac{\lambda'}{2r}\right)e^{-\lambda} - \frac{1}{r^2}\right] = 8\pi y(p_t - p_r). \quad (55)$$

Since  $e^{-\lambda} = 1 - 2m(r)/r$ , using eq. 52 we find

$$e^{-\lambda} = 1 - a - br^2 \equiv I_b^2(r). \quad (56)$$

In this section we will define the function  $I_b^2(x) \equiv 1 - a - bx^2$  to simplify our expressions. When  $b = 0$ , we will write  $I_0^2 \equiv 1 - a$ . Using the expression for  $e^{-\lambda}$  in eq. 55 and substituting for the pressure anisotropy we find

$$\left[br^4 - (1 - a)r^2\right] y'' + (1 - a)ry' - (a - c - dr^2)y = 0. \quad (57)$$

We give the full solution of eq. 57 with  $a, b, c, d \neq 0$  in Appendix B. Below, we will consider solutions obtained from choosing specific values for  $a, b, c$  and  $d$ .

**CASE I:** Stars with no crust ( $b = d = 0$ )

We first consider configurations where the energy density is given by

$$\rho = \frac{a}{8\pi r^2}. \quad (58)$$

For this density profile, the total mass is  $M = aR/2$  and

$$e^{-\lambda} = 1 - a. \quad (59)$$

Since for any static spherically-symmetric configuration we expect  $(2M/R)_{crit} \leq 1$ , we must have  $a < 1$ . (Also, the metric coefficient  $g_{rr}$  becomes infinite when  $a = 1$ ). A density profile with this spatial dependence on the radial coordinate was found to be an exact isotropic



solution of the TOV equation for the interior of ultra high-density neutron stars by Misner and Zapolsky [18]. Assuming that the neutron star core can be modeled as a relativistic Fermi gas, *i.e.*,  $p_r = \rho(r)/3$ , they found the density to be given by eq. 58, with  $a = 3/7$ . We note that the Misner-Zapolsky solution cannot be used to construct a complete star, since this would require the radius of the star to be infinite. Here, we want to construct stars with finite radii and density given by eq. 58 in the context of anisotropic pressure. Thus, we impose boundary conditions such that  $p_r(R) = 0$ . We also note that Herrera investigated anisotropic solutions with similar energy density, in the context of “cracking,” when perturbations in the fluid induce anisotropic stresses in the star [13,14]. However, we follow a different approach, focusing on the physical properties of static anisotropic solutions. With  $b = d = 0$ , eq. 57 reduces to an Euler-Cauchy equation,

$$(1 - a)r^2y'' - (1 - a)ry' + (a - c)y = 0. \quad (60)$$

The solutions of this equation divide into three classes, depending on the value of

$$q \equiv \frac{(1 + c - 2a)^{\frac{1}{2}}}{(1 - a)^{\frac{1}{2}}} \quad (61)$$

**Case I.1:**  $q$  is real

The solution for  $y$  is

$$y = A_+ \left(\frac{r}{R}\right)^{1+q} + A_- \left(\frac{r}{R}\right)^{1-q}, \quad (62)$$

with the constants  $A_+$  and  $A_-$  fixed by boundary conditions. For the case under consideration here ( $b = d = 0$ ), the boundary conditions are

$$e^{-\lambda(R)} = e^{\nu(R)} = I_0^2, \quad \text{and} \quad e^{\nu(R)} \frac{d\nu}{dr} \Big|_R = \frac{a}{R}. \quad (63)$$

Applying the boundary conditions we find

$$A_+ = \frac{I_0}{2} + \frac{1 - 3I_0^2}{4qI_0} \quad \text{and} \quad A_- = A_+(q \rightarrow -q). \quad (64)$$

The radial pressure for this case, after substituting the expressions for  $A_+$  and  $A_-$ , is

$$8\pi p_r = \frac{(3I_0^2 - 1)^2 - 4q^2 I_0^4}{r^2} \left[ \frac{R^{2q} - r^{2q}}{(3I_0^2 - 1 + 2qI_0^2)R^{2q} + (1 - 3I_0^2 + 2qI_0^2)r^{2q}} \right]. \quad (65)$$

We note that the boundary conditions automatically guarantee that  $p_r(R) = 0$ . The radial pressure is always greater than zero provided  $a < 2/3$  and  $a^2 > 4c(1 - a)$ . Since by definition  $a > 0$ , the second condition implies  $c > 0$ . Thus, this model does not allow for negative anisotropy. Further, since we are considering the case  $q > 0$ , we must impose the condition  $1 + c < 2a$ . Combining the two inequalities for  $a$  and  $c$ , we obtain,  $2a - 1 < c < a^2/4(1 - a)$ . Since we have  $0 < a < 2/3$  we find that  $0 < c < 1/3$ . We note that for the anisotropic case the maximum value of  $a$  is  $2/3$ , corresponding to a 33% increase when compared with the isotropic case ( $a = 3/7$ ). In figure 4 we plot the radial pressure,  $p_r$ , as a function of the radial coordinate  $r$ , for  $a = 3/7$  and several values of  $c$ . Note that for this choice of  $a$ , the inequality  $c < a^2/4(1 - a)$  imposes that  $c < 0.08$  for positive pressure solutions. This can be seen in the figure. For larger anisotropies, no static self-gravitating stable configuration is possible.

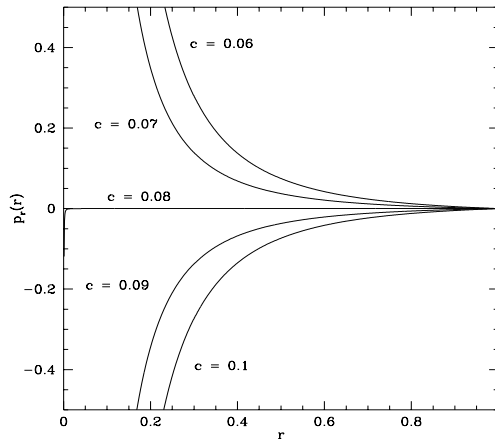


Fig. 4: Radial pressure as a function of  $r$  for  $\rho$  and  $(p_t - p_r) \propto r^{-2}$  and  $q$  real.

For  $r \ll R$ , we find

$$8\pi r^2 p_r = 3I_0^2 - 1 - 2qI_0^2. \quad (66)$$

Choosing  $a = 3/7$  we recover, in the limit  $c \rightarrow 0$ , the Misner-Zapolsky solution [18], with  $p_r = 1/(56\pi r^2) = \rho/3$ .

**Case I.2:**  $q = 0$

The solution for  $y$  with  $q = 0$  is

$$y(r) = A_s \left( \frac{r}{R} \right) + B_s \left( \frac{r}{R} \right) \ln \left( \frac{r}{R} \right), \quad (67)$$

where the constants  $A_s$  and  $B_s$  are determined from the boundary conditions. We find

$$A_s = I_0 \quad \text{and} \quad B_s = \frac{1 - 3I_0^2}{2I_0}. \quad (68)$$

The radial pressure is given by

$$8\pi r^2 p_r = 3I_0^2 - 1 + \frac{(1 - 3I_0^2)}{1 + \frac{(1 - 3I_0^2)}{2I_0^2} \ln \left( \frac{r}{R} \right)}. \quad (69)$$

The radial pressure is positive provided  $a < 2/3$ . Since we are considering the case  $q = 0$ , we must require  $c = 2a - 1$  and thus  $-1 < c < 1/3$ .

**Case I.3:**  $q$  is imaginary

The solution for  $y(r)$  with  $q$  imaginary is

$$y = \frac{r}{R} \left\{ A_s \cos \left[ u \ln \left( \frac{r}{R} \right) \right] + B_s \sin \left[ u \ln \left( \frac{r}{R} \right) \right] \right\} \quad (70)$$

with  $u = |q|$ . For  $A_s$  and  $B_s$  we find

$$A_s = I_0, \quad \text{and} \quad B_s = \frac{1 - 3I_0^2}{2uI_0}. \quad (71)$$

The radial pressure is given by

$$8\pi r^2 p_r = 3I_0^2 - 1 + \frac{2uI_0^2 \left[ 1 - 3I_0^2 - 2uI_0^2 \tan \left( u \ln \left( \frac{r}{R} \right) \right) \right]}{(1 - 3I_0^2) \tan \left( u \ln \left( \frac{r}{R} \right) \right) + 2uI_0^2}. \quad (72)$$

An analysis of eq. 72 shows that  $p_r > 0$  provided that  $a < 2/3$  for any  $c$ . Also, since we are considering the case  $q$  imaginary here, we require that  $c < 2a - 1$ .

**Case II:** Including a Crust ( $a, b, c \neq 0, d = 0$ )

We will now derive solutions of the field equations with the density profile given by eq. 52. This density profile is essentially a combination of the two profiles ( $\rho = \text{const}$  and  $\rho \propto 1/r^2$ ) that we have studied so far. We may think of this situation as modelling an ultradense core immersed in a background of constant density; at large distances from the core ( $r_c^2 \gg a/3b$ ), the constant density shell dominates the energy density. As in Case I, we impose boundary conditions such that  $p_r(R) = 0$ .

For this density profile,

$$e^{-\lambda} = I_b^2(r) , \quad (73)$$

and the equation for  $y = e^{\frac{\nu}{2}}$  is

$$\left((1-a)r^2 - br^4\right) y'' - (1-a)ry' + ay = 8\pi r^2 y(p_t - p_r). \quad (74)$$

The boundary conditions are

$$y(R) = I_b^2(R) \quad \text{and} \quad y'(R) = \frac{1 - I_b^2(R)}{2RI_b(R)}. \quad (75)$$

Here, we have chosen the ansatz for the anisotropic pressure to be the same as the case with  $b = 0$ , that is, we do not include a constant contribution to the anisotropy ( $d = 0$  in eq. 53). The general solution for  $d \neq 0$  is given in Appendix B. As with the case above with  $b = 0$ , there are three classes of solutions depending on the value of

$$q = \frac{(1 - 2a + c)^{\frac{1}{2}}}{(1 - a)} . \quad (76)$$

### Case II.1 $q$ real

For  $q$  real ( $1 + c > 2a$ ) the solution is

$$y = A_+ \left(\frac{r}{R}\right)^{1+q} \left[\frac{I_0 + I_b(r)}{I_0 + I_b(R)}\right]^{-q} + A_- \left(\frac{r}{R}\right)^{1-q} \left[\frac{I_0 + I_b(r)}{I_0 + I_b(R)}\right]^{+q} . \quad (77)$$

Using the boundary conditions as before we find

$$A_+ = \left[ \frac{(3I_b^2(R) - 1)}{4qI_0} + \frac{I_b(R)}{2} \right] \quad \text{and} \quad A_- = A_+(q \rightarrow -q). \quad (78)$$

The radial pressure is given by

$$8\pi r^2 p_r = \frac{[3I_b^2(r) - 1 - 2qI_0I_b(r)] + [3I_b^2(r) - 1 + 2qI_0I_b(r)] \left(\frac{A_-}{A_+}\right) \left(\frac{r}{R}\right)^{-2q} \left(\frac{I_0+I_b(r)}{I_0+I_b(R)}\right)^{2q}}{1 + \left(\frac{A_-}{A_+}\right) \left(\frac{r}{R}\right)^{-2q} \left(\frac{I_0+I_b(r)}{I_0+I_b(R)}\right)^{2q}}. \quad (79)$$

We note that when  $b = 0$ , we recover the solution with no crust. Also, if we take  $a = 0$  and  $b \neq 0$ , we have a new class of anisotropic solutions with constant density, and anisotropy proportional to  $r^{-2}$ .

### Case II.2: $q = 0$

When  $q = 0$ , the solution is

$$y(r) = e^{\nu(r)/2} = A_s \left(\frac{r}{R}\right) + B_s \left(\frac{r}{R}\right) \ln \left\{ \frac{[I_0 + I_b(r)][I_0 - I_b(R)]}{[I_0 - I_b(r)][I_0 + I_b(R)]} \right\} \quad (80)$$

with

$$A_s = I_b(R), \quad \text{and} \quad B_s = \frac{(3I_b^2(R) - 1)}{4I_0}. \quad (81)$$

Here, the radial pressure is given by

$$8\pi r^2 p_r = 3I_b^2(r)^2 - 1 - 4I_b(r)I_0B_s e^{-\frac{\nu}{2}}. \quad (82)$$

### Case II.3: $q$ is imaginary

When  $q$  is imaginary the solution is

$$y = \left(\frac{r}{R}\right) \left[ A_s \frac{\sin(s \ln F(r))}{\sin(s \ln F(R))} + B_s \frac{\cos(s \ln F(r))}{\cos(s \ln F(R))} \right], \quad (83)$$

with

$$A_s = 2I_b(R) \tan(F(R)) \tan(2F(R)) - \frac{(1 - 3I_b^2(R))}{sI_0} \tan(2F), \quad B_s = I_b(R) - A_s, \quad (84)$$

and

$$F(x) = s \ln \left[ \frac{(1-a)^{\frac{1}{2}} + (1-a-bx^2)^{\frac{1}{2}}}{(1-a)^{\frac{1}{2}}} \right]. \quad (85)$$

We intend to investigate numerically the allowed range of the parameters  $a$ ,  $b$ ,  $c$ , and  $d$ , as well as the stability of these solutions, in a forthcoming publication.

## V. CONCLUSIONS

We have presented two broad classes of general relativistic exact solutions of spherically symmetric stellar configurations exhibiting anisotropic pressure. Our motivation was to explore the changes in the general properties of the stars induced by varying amounts of anisotropy. In particular, to each of the solutions we have demonstrated that anisotropy may indeed change the critical mass and surface redshift of the equilibrium configurations, results which we believe are of interest to the astrophysical community and will stimulate further investigation. It is an open question if, indeed, anisotropy is relevant for compact objects, as, for example, ultradense neutron stars. We have motivated our results based on past work on this subject, where isotropic equations of state are at best a reasonable hypothesis. Given that we do not have as of yet a complete understanding of the physical processes controlled by strong interactions in ultradense matter [3], it is wise to keep an open mind to the possibility that anisotropic stresses do occur. Furthermore, hypothetical compact objects made of gravitational bound states of bosonic fields, the so-called boson stars, are naturally anisotropic [19]. These objects have been extensively studied in the literature, as they represent an interesting new class of compact objects whose stability against gravitational collapse comes from a combination of Heisenberg's uncertainty principle and model-dependent self-interactions. They may also have some connection with dark matter, if perturbations on a fundamental scalar field lead to instabilities which trigger the gravitational collapse of overdense regions.

We have divided our work into two classes of solutions, those with a constant energy density and those with an energy density falling as  $r^{-2}$ . Within each of these classes we

presented several possible cases, which we hope approximate to some extent possible realistic objects, including a combined situation where the star's energy density has an ultradense interior ( $\rho \propto r^{-2}$ ) immersed in a shell of constant density. We intend to study the stability of these solutions against radial perturbations, as well as provide a detailed numerical analysis of the allowed parameter space, in a future work. We also added two appendices, one proving the equality between the Tolman and the Schwarzschild mass formulas and the other providing the general solution for the  $\rho \propto r^{-2} + \text{const}$  case in terms of hypergeometric functions.

## VI. ACKNOWLEDGEMENTS

We would like to thank Joseph Harris, Paul Haines, and especially Vincent Moncrief for their interest in our work and many useful suggestions. KD thanks Dartmouth College for a Dartmouth Fellowship. MG was supported in part by National Science Foundation Grants PHY-0070554 and PHYS-9453431.

## VII. APPENDIX A

Here we will establish the equivalence of the Tolman and Schwarzschild mass formulas for static spherically symmetric spacetimes with anisotropic pressure. The general expression for the Tolman mass formula is

$$M_T = \int (2T_0^0 - T_\nu^\nu) (-g)^{\frac{1}{2}} d^3x . \quad (86)$$

Here we have

$$T_0^0 = \rho \quad \text{and} \quad T_\nu^\nu = \rho - p_r - 2p_t . \quad (87)$$

Substituting the values of  $T_0^0$  and  $T_\nu^\nu$  in equation 86 we have

$$M_T = \int_0^R 4\pi r^2 e^{\frac{\nu+\lambda}{2}} (\rho + p_r + 2p_t) dr . \quad (88)$$

Let

$$I_1 = \int_0^R 4\pi r^2 \rho e^{\frac{\nu+\lambda}{2}} dr \text{ and } I_2 = \int_0^R 4\pi r^2 (p_r + 2p_t) e^{\frac{\lambda+\nu}{2}} dr ; \quad (89)$$

then,

$$M_T = I_1 + I_2. \quad (90)$$

Defining

$$m(r) = \int_0^r 4\pi r^2 \rho dr , \quad (91)$$

the Schwarzschild mass is given by

$$M_S = m(R) . \quad (92)$$

Consider the integral  $I_1$ . Performing an integration by parts we find

$$I_1 = \left[ m e^{\frac{\lambda+\nu}{2}} \right]_0^R - \int_0^R m \left( e^{\frac{\lambda+\nu}{2}} \right)' dr. \quad (93)$$

The first term evaluates to  $M_S$ , since  $m(0) = 0$  and, at  $r = R$ ,  $\lambda + \nu = 0$ . From the field equations it follows that

$$\frac{(\lambda + \nu)'}{2} = \frac{4\pi r^2 (\rho + p_r)}{(r - 2m)}. \quad (94)$$

Substituting this expression in equation 93 we find

$$I_1 = M_S - \int_0^R \frac{4\pi m r^2 (\rho + p_r)}{(r - 2m)} e^{\frac{\lambda+\nu}{2}} dr. \quad (95)$$

Next we consider the integral  $I_2$ . Using the generalized TOV equation we can substitute for  $p_t$  and write

$$I_2 = \int_0^R 4\pi r^2 e^{\lambda+\nu} \left( 3p_r + r \frac{dp_r}{dr} + \frac{(4\pi p_r r^3 + m)(\rho + p_r)}{(r - 2m)} \right) dr . \quad (96)$$

We will rewrite this as

$$I_2 = I_{2a} + I_{2b} , \quad (97)$$

with



$$I_{2a} = \int_0^R 4\pi r^2 (3p_r) e^{\frac{\lambda+\nu}{2}} dr , \quad (98)$$

and

$$I_{2b} = \int_0^R 4\pi r^2 \left( r \frac{dp_r}{dr} + \frac{(4\pi p_r r^3 + m)(\rho + p_r)}{(r - 2m)} \right) e^{\frac{\lambda+\nu}{2}} dr . \quad (99)$$

Integrating  $I_{2a}$  by parts we find

$$I_{2a} = \left[ 4\pi r^3 p_r e^{\frac{\lambda+\nu}{2}} \right]_0^R - \int_0^R 4\pi r^3 \left( \frac{dp_r}{dr} + \frac{p(\lambda' + \nu')}{2} \right) e^{\frac{\lambda+\nu}{2}} dr . \quad (100)$$

The first term of this equation is equal to zero, since  $p_r(R) = 0$ , and substituting for  $\nu' + \lambda'$  from equation 94 we find that

$$I_{2a} = - \int_0^R 4\pi r^2 \left( r \frac{dp_r}{dr} + \frac{4\pi p_r r^3 (\rho + p_r)}{(r - 2m)} \right) e^{\frac{\lambda+\nu}{2}} dr . \quad (101)$$

By adding  $I_{2a}$  and  $I_{2b}$ , we get

$$I_2 = \int_0^R 4\pi r^2 \left( \frac{m(\rho + p_r)}{(r - 2m)} \right) e^{\frac{\lambda+\nu}{2}} dr . \quad (102)$$

Finally  $I_1$  plus  $I_2$  gives

$$M_T = M_S . \quad (103)$$

This demonstrates the equivalence of the Tolman and Schwarzschild mass formulas for static spherically symmetric spacetimes with anisotropic pressures.

## VIII. APPENDIX B

The solution for eq. 57 with  $a, b, c, d \neq 0$ ,  $a \neq 1$  and boundary conditions given by eq. 75 is

$$y = A_+ \left( \frac{r}{R} \right)^{1+q} F_+(\tilde{r}) + A_- \left( \frac{r}{R} \right)^{1-q} F_-(\tilde{r}) \quad (104)$$

Here  $\tilde{r} = \frac{br}{1-a}$  and  $F$  is the hypergeometric function:

$$F = F(\alpha, \beta, \gamma, x) = 1 + \sum_{k=1}^{\infty} \frac{(\alpha)_k (\beta)_k}{(\gamma)_k} \frac{x^k}{k}, \quad (\alpha)_k = \alpha(\alpha+1)\dots(\alpha+k-1) , \quad (105)$$

$$\frac{d}{dx}F(\alpha, \beta, \gamma, x) = F' = \frac{\alpha\beta}{\gamma}F(\alpha + 1, \beta + 1, \gamma + 1, x) \quad (106)$$

and

$$F_+ = F(\alpha_+, \beta_+, \gamma_+, \tilde{r}), \quad F_- = F_+(q \rightarrow -q) \quad (107)$$

with

$$\begin{aligned} \alpha_+ &= \frac{1}{4}[1 + 2q - (\frac{b-4d}{b})] , \\ \beta_+ &= \frac{1}{4}[1 + 2q + (\frac{b-4d}{b})] , \\ \gamma_+ &= \frac{1}{4}(1 + q) , \\ q &= \left( \frac{1 - 2a + c}{1 - a} \right)^{\frac{1}{2}} . \end{aligned} \quad (108)$$

Using the boundary conditions we find

$$A_+ = \frac{1 - 3I_b^2(R) - 2qI_b^2(R) + 2I_b^2(R)\{\ln[F_-(\tilde{R})]\}'}{2I_b(R)\{qF_+(\tilde{R}) + R[F_+(\tilde{R})]' - RF_+(\tilde{R})\{\ln[F_-(\tilde{R})]\}'\}}, \text{ and } A_- = A_+(q \rightarrow -q). \quad (109)$$

The radial pressure is given by

$$\begin{aligned} 8\pi r^2 p_r &= \frac{3I_b^2(r) - 1 + 2qI_b^2(r) + 2I_b^2(r)(\ln[F_+(\tilde{r})])'}{1 + \frac{A_-}{A_+} \frac{F_-(\tilde{r})}{F_+(\tilde{r})} (\frac{r}{R})^{-2q}} \\ &+ \frac{(3I_b^2(r) - 1 - 2qI_b^2(r)) \frac{A_-}{A_+} (\frac{r}{R})^{-2q} (\frac{F_-(\tilde{r})}{F_+(\tilde{r})} + 2g^2 \frac{(F_-(\tilde{r}))'}{F_+(\tilde{r})})}{1 + \frac{A_-}{A_+} \frac{F_-(\tilde{r})}{F_+(\tilde{r})} (\frac{r}{R})^{-2q}} . \end{aligned} \quad (110)$$

## REFERENCES

- [1] D. D. Clayton, *Principles of Stellar Evolution and Nucleosynthesis*, (The University of Chicago Press, Chicago, 1983).
- [2] R. Kippenhahn and A. Weigert, *Stellar Structure and Evolution*, (Springer-Verlag, Berlin, 1991).
- [3] N. K. Glendenning, *Compact Stars: Nuclear Physics, Particle Physics and General Relativity*, (Springer-Verlag, Berlin, 1997); H. Heiselberg and M. H.-Jensen, Phys. Rep. **328**, 237 (2000).
- [4] M. Ruderman, Annu. Rev. Astron. Astrophys., **10**, 427 (1972).
- [5] V. Canuto, Annu. Rev. Astron. Astrophys., **12**, 167 (1974).
- [6] For comprehensive reviews see, A. R. Liddle and M. S. Marsden, Int. J. Mod. Phys. **D1** 101, (1992); P. Jetzer, Phys. Rep. **220**, 163 (1992); E. W. Mielke and F. E. Schunck, in *Proceedings of 8th M. Grossmann Meeting*, T. Piran (ed.), (World Scientific, Singapore, 1998).
- [7] R. Sawyer and D. Scalapino Phys. Rev. **D7**, 382 (1973).
- [8] R. L. Bowers and E. P. T. Liang, Ap. J. **188**, 657 (1974).
- [9] J. Ponce de Leon, J. Math. Phys., **28**, 1114 (1987).
- [10] M. Gokhroo and A. Mehra Gen. Rel. Grav., **26**, 75 (1994).
- [11] H. Bondi, Mon. Not. R. Astron. Soc. **259**, 365 (1992).
- [12] E. S. Corchero, Clas. Quantum Grav. **15**, 3645 (1998).
- [13] L. Herrera, Phys. Lett. **A 165**, 206 (1992).
- [14] L. Herrera and N. O. Santos, Phys. Rep., **286**, 53, 1997.
- [15] S. Weinberg, Gravitation and Cosmology, (Wiley, New York, 1972).

- [16] R. C. Tolman, Phys. Rev. **35**, 875 (1930).
- [17] J. B. Hartle and K. Thorne, Ap. J., **153**, 803 (1968)
- [18] C. Misner and H. Zalopsky, Phys. Rev. Lett., **12**, 635 (1964).
- [19] M. Gleiser, Phys. Rev. **D38**, 2376 (1988); M. Gleiser and R. Watkins, Nucl. Phys. **B319**, 733 (1989).